Jurnal Kejuruteraan 34(3) 2022: 395-400
https://doi.org/10.17576/jkukm-2022-34(3)-06

Determination of Thermal Expansion Coefficient for Ball Grid Array using Digital Image Correlation

Yat Sheng Kong[a*] & Liam Crosbie[b]

[a]*Quantarad Technologies Sdn Bhd, B-2, 18, Jalan PJU 1A/3, Taipan Damansara 2, 47301 Ara Damansara, Selangor, Malaysia*
[b]*Dantec Dynamics A/S, Kaessbohrerstrasse 18, 89077 Ulm, Germany*

**Corresponding author: yatsheng.kong@quantarad.com*

Received 25 March 2021, Received in revised form 26 August 2021
Accepted 27 September 2021, Available online 30 May 2018

ABSTRACT

This paper presents the analysis of coefficient of thermal expansion (CTE) of solder ball on a ball grid array (BGA) through digital image correlation (DIC) technique. The assessment of thermal mechanical properties of semiconductor component is a main challenge due to the sensitivity of micro-scale components to heat. However, the CTE analysis of BGA is significant to address the issues of thermal mismatch strains which lead to failure. Meanwhile, the measurement of solder ball heat expansion is in microscale and heated conditions where the traditional method of strain measurements is ineffective. In this analysis, a micro DIC system was used to measure the strain value of solder balls when it was subjected to temperature loading in a heating stage. The actual temperature of the solder ball was measured using a thermocouple inside the heating stage to ensure uniformity of the temperature. The measured strain during the specific temperature was obtained and plotted for CTE using linear analysis. The average value of CTE for the measured solder ball was 27.33 × 106 / oC. The results indicated that the measurement was close to the reference value of solder ball CTE. This analysis provides a reliable analysis of BGA using a developed DIC method.

Keywords: Digital image correlation, Coefficient of Thermal Expansion, Solder ball, Thermal-mechanical

INTRODUCTION

In micro-electronics industry, thermally induced stress is a challenge during the fabrication processes of ball grid array (BGA) or printed circuit board (PCB). The thermal expansion of components is significant due to the non-uniformity deformation which will lead to failure (Sun et al. 2006). The thermal-mechanical properties of micro-electronic components are usually determined using a parameter known as coefficient of thermal expansion (CTE) where this parameter is used for component design, structural response, and material selections. To obtain the CTE value of a design, the most traditional ways are through finite element simulations or experimental procedures (Dudescu et al. 2013)

To resolve the problems of CTE measurement, a non-contact optical measurement technique is required. One of the full field optical technique for CTE measurement is electronic speckle pattern interferometry (Dudescu et al. 2006) This technique is sensitive to testing environmental such as vibration and convection current flows around the specimen, especially when focusing into micro-scale. Another widely used non-contact optical technique in CTE analysis is known as digital image correlation (DIC). DIC is a non-contact optical technique which used to measure contour, strain, vibration, and deformation of almost all materials. The DIC method was used to measure CTE of polymeric materials through linear fittings (Choube & Ghaffarian 2016). In addition, DIC was also used to measure the CTE of glass-fiber cloth epoxy laminate for thermal expansion mismatch (Hohjo et al. 2019). The measurement of the CTE for glass-fiber cloth epoxy laminate was consistent at temperature up to 180˚C and it was not affected by contact deviations.

For microelectronic components, DIC was used to measure in-plane displacement and out of plane warpage in a single measurement (Niu et al. 2018). DIC was also used to measure CTE of BGA package for increasing package reliability during soldering reflow (Rovitto & Villa 2019). Instead of thermal mismatch, the fatigue behaviour of BGA was also investigated using different thermal cycle as loading (Pham et al. 2020). An analysis has been performed by Cai et al. (2020) to study the package warpage using Confocal, DIC, Shadow Moire and digital fringe projection where the DIC method has advantages in inspecting the in-plane and out of plane deformation. Additionally, DIC was used to perform heat-related fatigue reliability analysis of solder joints in microelectronic packages (Sun & Pang 2008). The results of the DIC were validated and comparable with finite element analysis.

The aim of this work is to utilize DIC technique in obtaining the CTE of two solder balls on a BGA under heated condition. The main challenge of this analysis was to provide in-situ CTE measurement of a solder ball with the accuracy up to micro-scale from -50 to 80˚C. The heating process of the solder ball is required to remain consistent in which a conduction-base heating stage was used. The obtained CTE was compared with a literature reference value. This experimental works contributes to field of thermo mechanical for microelectronics using a DIC systems with an integrated microscope. In addition, a good prediction of component CTE during thermal process becomes significant for reducing package warpage which reduce the risk of thermo mechanical failure.

METHODOLOGY

In this analysis, a BGA with solder ball joint on the surface was selected for thermal expansion analysis. The selected BGA is made of tin-lead material with a surface size of 25 × 25 mm. The experimental setup of the BGA is shown in Figure 1(a). Since the main objective of this work is to measure thermal expansion of the BGA, an additional thermocouple was applied to measure the actual temperature of the component. The diameter of the solder ball of the BGA was 0.5 mm with the height of 0.35 mm. The geometry measurement of the solder ball using DIC system is shown in Figure 1(b). As observed, the BGA is sprayed with white coating and a contrasting paint for speckle pattern was applied on top of the white paint. The basic principle of DIC was to calculate the displacement field of a deforming body by tracking the position change of random speckles pattern on the component surface (McCormick & Lord 2010). For a planar analysis, it was assumed that a small point on the body moves to a new location after deformation.

The greyscale distribution between two points was estimated using a correlation technique. The correlation technique was based on pseudo-affine coordinate's transformation of object points where it tracked the observed grey value patterns for each camera and transforms corresponding facet positions into 3D coordinates for each step (Trebuna et al. 2013). The transformation parameters of potential translation, stretch, shear and distortion were determined by minimizing the distance between the detected grey pattern of the reference image and second image through photogrammetric corrections. The intensity change of points during loading was also integrated into the photogrammetric correction. When the initial displacement vectors and contour of points were identified, the strain was computed from these data. The strain data was obtained through differentiation of adjacent displacement points or correlation of local facets curve.

A DIC system was normally used for 3D and sensitive warpage, thermal expansion measurement and strain analysis of materials under heating or cooling conditions. The DIC systems used in this analysis was Dantec Dynamics DIC. The measurement could be performed non-contacted, on the whole measuring area and on nearly any material. The field of view of the system can be adjusted down to square millimetres. For this specific instrument setup, the measurement range was from 1 to 15 mm sample size. Despite the BGA size was 25 × 25 mm, the solder ball on the BGA was only around 500 µm. The achieved field of view (FoV) for this measurement was about 2 mm which including 2 solder balls simultaneously. The DIC machine setup is shown in Figure 2 where this instrument consisted of 2 high resolution cameras with 5.1 Mega pixel and 23 frames per second. The camera module was completely integrated into the DIC systems for optimization of material testing system. For this microscale measurement, a stereo microscope was installed with the camera for sub-micron measurement. With the microscope, the focus level of the DIC system was enhanced to measure solder ball deformation.

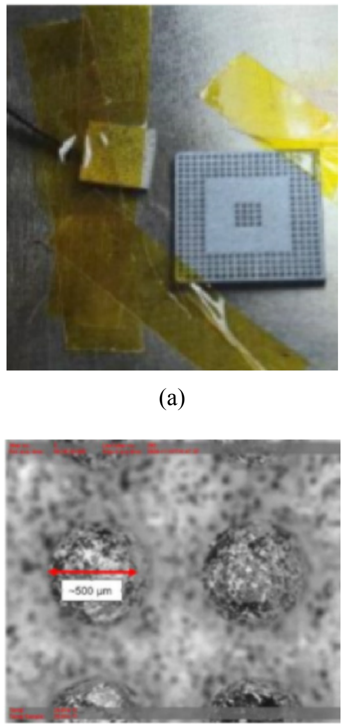

(a)

(b)

FIGURE 1. Preparation of sample (a) painted specimen (b) reference image of BGA

The accuracy of measurement of CTE of isotropic materials depends on the resolution of DIC systems in measuring deformation and temperature control on the specimen. For thermal expansion analysis, it was important to ensure that no external loadings or mechanical restraints on the sample which could lead to erroneous measurements. The CTE could be obtained when the strain value and temperature change were obtained (Dudescu et al. 2013). Using the DIC measuring technique, this presumes recording of gray patterns at two different temperatures, T1 and T2. Using specific image processing software one can determine the full field distributions of strain and displacement belonging to ΔT. The equation of CTE is given as below:

$$\alpha = \frac{\varepsilon}{\Delta T} \quad (1)$$

where the α is the CTE value, ε is the strain value and ΔT is the temperature change. Another critical aspect that should be carefully considered was the temperature dependence of the CTE. Although CTE is a function of temperature, it can be considered as a constant in large temperature range (Choube & Ghaffarian 2016).

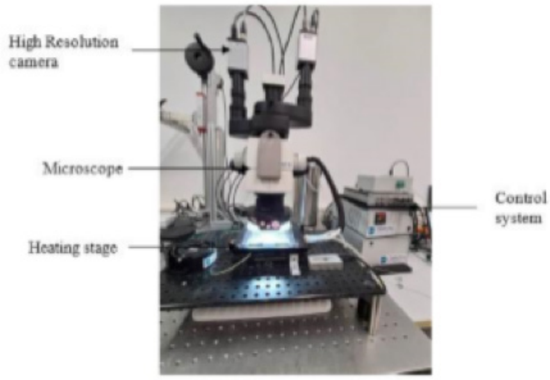

FIGURE 2. Experimental setup for strain and temperature measurement

The 3D surface measurements use one, multicamera DIC setup to measure either side of a specimen in a single coordinate system. The multicam DIC systems enable the real time measurement of bi-planar measurement of system. Prior to the measurement, a setup on the detected image was required. For linear CTE analysis, virtual strain gauge was applied on the sample specimen. In this case, one line and one circle were created for each of the solder ball as shown in Figure 3. The straight line captures the in-plane strain and the circle measure the strain of the selected region. The line gauge measured Euclidean length while the circle gauge was calculated over surface or border. The circle featuring a diameter superposed on images observed in a displacement map. The obtained displacements were cross correlated, and the strain values were derived from the displacement. Due to the limited field of view (FoV), the measurement was only taken for 2 solders simultaneously which labelled as solder ball 1 and 2, respectively.

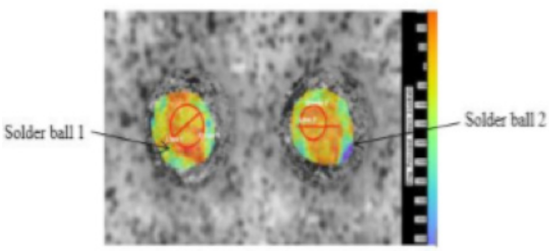

FIGURE 3. Generated measurement line and circle

The heating process of the BGA was conducted in a heating stage with electronic controller where the measurement could be done from room temperature up to 300˚C and reduced to -40˚C. For this BGA, the operating temperature of the BGA was from -40 to 70˚C (Serebreni et al. 2017). Hence, the experimental temperature profile was controlled from -50 to 80˚C with a temperature change at 25˚C as shown in Figure 4. For this heating process, it took a total of 6,000 s to complete the experiment. The heating stage provided heating through conduction to the BGA and cooling through liquid nitrogen. This temperature profile was used as input to the heating stage and the actual temperature of BGA was measured using a thermocouple. The signals were given to the heating stage when the sample reached the desired temperature for accurate temperature control.

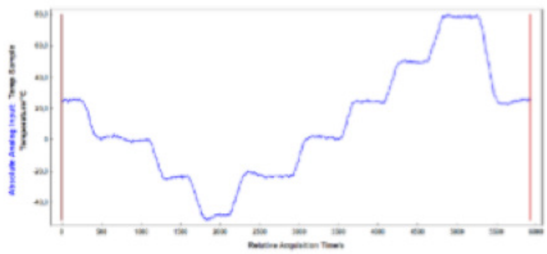

FIGURE 4. Heating curve for BGA

RESULTS AND DISCUSSION

The CTE analysis required deformation and temperature data collection on the solder ball. For actual temperature measurement, a thermocouple was applied on the BGA for real time data recording. As the outcome, the temperature curve for the solder ball 1 and 2 from thermocouple measurement is shown in Figure 5. Initially, the temperature was reduced through nitrogen liquid, and data was recorded for every 25˚C changes. In this analysis, the first hour was a cooling process where the temperature of the BGA was reduced. After 30 minutes, the temperature has reached -50˚C and data was collected. The average value for this temperature range was obtained. Subsequently, the temperature was gradually increased to 80˚C after 30 minutes of heating before cooled down to ambient

Using the DIC technique, measurement of strain if the solder ball could be visualised in different contours as shown in Figure 6. As observed, the maximum principal strain during temperature at 78.12˚C was 977 µstrain. The measurement of small strain value induced on the solder ball during heating stage is accompanied by noise and decreased accuracy. Hence, to obtain the actual CTE, linear regression was required for the data fittings (Lee et al. 2016). For the line virtual strain gauge on solder ball 1, the strain-temperature curve is plotted as shown in Figure 7. As observed, the heating and cooling process has formed a hysteresis curve where the energy was dissipated. In addition, at the temperature of above 20˚C, the deformation of the solder ball become larger and the strain difference between heating and cooling was increased. On the other hand, the measurement of CTE using circle virtual strain gauge is shown in Figure 8. The CTE curve was more consistent when compared to line virtual strain gauge measurement.

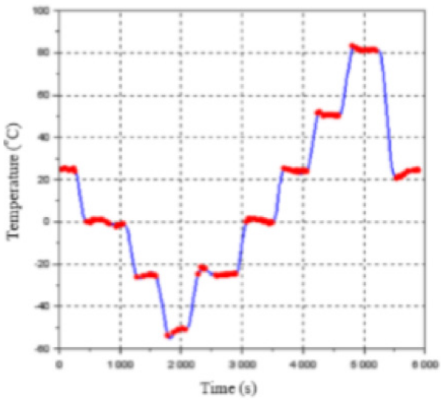

FIGURE 5. Temperature curve of solder ball 1 during thermal loading

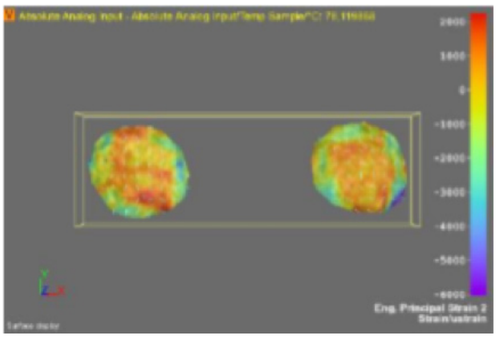

FIGURE 6. Strain contour of solder ball at 78°

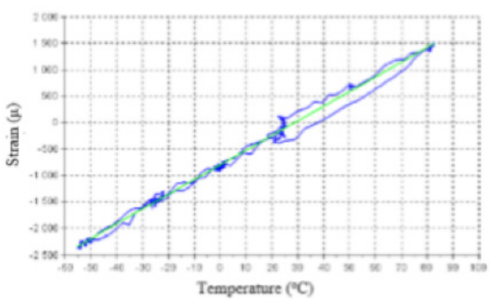

FIGURE 7. Variation of temperature of the thermal strains using line for solder ball 1

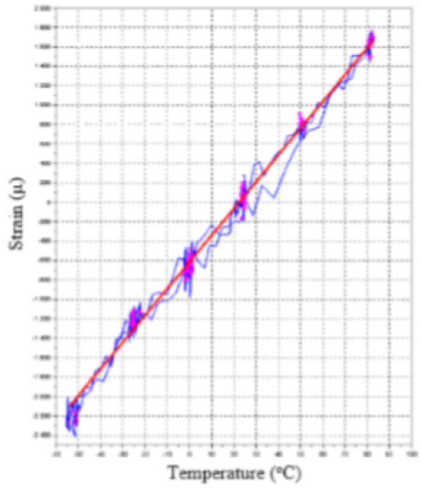

FIGURE 8. Variation of temperature of the thermal strains using circle for solder ball

The CTE was obtained through using a linear fitting between the strain value with respect to their temperature value. Based on the linear fitting, the regression was obtained for the line and circle for solder ball 1 as below:

$$\varepsilon_1 = 27.828 * T - 682.46 \quad (2)$$

$$\varepsilon_2 = 27.534 * T - 619.90 \quad (3)$$

where ε_1 is the line gauge strain value and ε_2 is the circle gauge strain value for solder ball 1. The obtained CTE value using line gauge was 27.82 × 10-6 /ºC while the CTE value using circle was 27.53 × 10-6 /ºC. The CTE reference value of solder ball is 25 × 10-6/ºC (Lee et al. 2003). Based on the solder ball CTE reference value, the difference between line and circle gauge was 11.3 and 10.1% respectively. For numerical simulation and experimental results, the difference between 20% is considered as acceptable (Zhang et al. 2007). Hence, the measurement outcome is acceptable. It is noteworthy to mention that the reference CTE value was a general guide to solder ball in which the actual design of solder could be varied.

For solder ball 2, linear fitting was performed for both line and circle grid data as shown in Figures 9 and 10, respectively. For the linear regression, the gradient and intercept were obtained as follows:

$$\varepsilon_3 = 27.155 * T - 790.57 \quad (4)$$

$$\varepsilon_4 = 26.850 * T - 651.17 \quad (5)$$

where ε_3 is the line gauge strain value and ε_4 is the circle gauge strain value for solder ball 2. The CTE for solder ball using line gauge was 27.152 × 10-6 /°C while the CTE for circle gauge was 26.850 × 10-6 /°C. The difference between line and circle gauge measurement with reference value was 8.61 and 7.4% respectively. This shown that the measured CTE were close to the expected value.

The CTE value for all four measurement gauges were fall within the expected range. Additionally, both line and circle gauges are suitable for CTE calculation where the obtained coefficient of correlation R^2 were above 0.90. The average CTE value for the measurements were 27.334 × 10-6 /°C where a difference of 9.34% with reference value was obtained. Currently, the measurement of CTE for solder ball is still a big challenge due to the consistency of temperature during heating. Another issue to be concerned was the vibration of the camera when heated air flow was supplied to the sample which could lead to blur image. Additionally, the attachment of microscope to DIC systems has caused the image detection more sensitive. Without a stable image, the measurement of CTE could be inaccurate which lead to thermal mismatch failure. Hence, the method demonstrated in this work offers a solution for CTE measurement of microelectronic components with good accuracy.

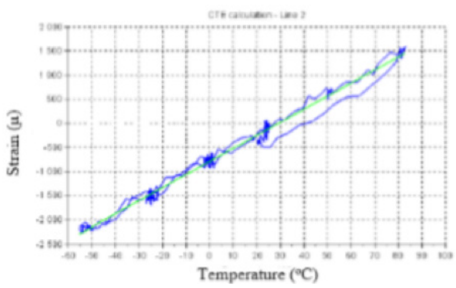

FIGURE 9. Variation of temperature of the thermal strains using circle for solder ball

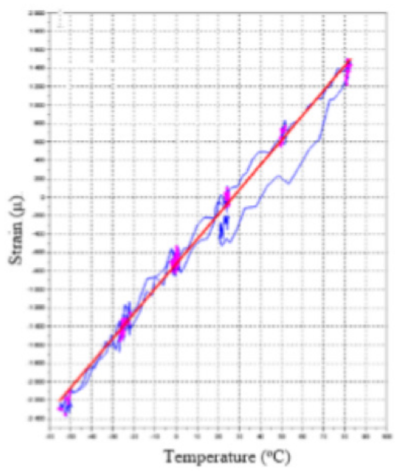

FIGURE 10. Variation of temperature of the thermal strains using circle for solder ball 2

CONCLUSION

The CTE value of solder ball from a BGA was successfully determined using DIC method with good accuracy. The average CTE of the solder ball from DIC measurement was 27.334×10-6 /˚C after a linear fitting was implemented on all the data. The obtained CTE has 9.34% deviation from a literature reference. This implied that the micro-scale measurement of the solder ball under heated condition was good. With the known CTE of solder ball, the design of BGA is facilitated. This research serves to provide a solution for CTE measurement of solder ball which prevent the thermal mismatch or failure of microelectronic components.

ACKNOWLEDGEMENT

This work was supported by the Universiti Teknologi MARA (UiTM) Cawangan Sarawak, Malaysia.

DECLARATION OF COMPETING INTEREST

None

REFERENCES

Cai C., Pan K., Yang J., Park. S. 2020. Comparative analysis of package warpage using confocal method and digital image correlation, *2020 19th IEEE Intersociety Conference on Thermal and Thermomechanical Phenomena in Electronic Systems (ITherm)*, USA.

Choube A, Ghaffarian R. 2016. FEA and analysis for BGA/CGA assemblies under thermal cycling. Proceedings of the SMTA International: 509 – 517, USA.

Dudescu M, Botean A, Hardao. M. 2013. Thermal expansion coefficient determination of polymeric materials using digital image correlation. *Materiale Plastice* 50(1): 55 – 59.

Dudescu M, Naumann J, Stockmann M, Nebel S. 2006. Characterisation of thermal expansion coefficient of anistropic materials by ESPI. *Strain* 42(3): 197 – 206.

Hohjo H, Kojima Y, Ohta T, Makino H. 2019. Determination of non-uniform microscopic distributions of thermal strains in glass-fiber cloth/epoxy laminates using DIC. *Experimental Technique* 43: 405 – 414.

Lee T.I., Kim M.S., Kim. T.S. 2016. Contact-free thermal expansion measurement of very soft elastomers using digital image correlation. *Polymer Testing* 51: 181 – 189.

McCormick N. & Lord J. 2010. Digital Image Correlation, *Materialstoday* 13(12): 52 – 54.

Niu Y, Wang J., Shao S., Wang H., Lee H., Park. S.B. 2018. A comprehensive solution for electronic packages reliability assessment with digital image correlation method. *Microelectronics reliability* 87: 81 – 88.

Pham V.L., Xu J., Pan K., Wang J., Park S., Singh C., Wang. H. 2020. Investigation of underfilling BGAs packages – thermal fatigue, *2020 IEEE 70th Electronic Components and Technology Conference (ECTC)*, USA.

Rovitto M. & Villa. C.M. 2019. Novel methodology for real time thermal expansion characterisation on ball grid array substrate stack up materials. *Microelectronics reliability* 100-101: 113478.

Serebreni M., Wilcoxon R., Hillman D., Blattau N., Hillman C. 2017. The effect of improper conformal coating on SnPb and Pb-free BGA solder joints during thermal cycling. *Experiments and modelling, 33rd Thermal Measurement, Modeling & Management Symposium (SEMI-THERM),* USA.

Sun Y, Pang JHL, Shi X, Tew JWR. 2006. Thermal deformation measurement by digital image correlation method, *Thermal and Thermomechanical Proceedings 10th Intersociety Conference on Phenomena in Electronics Systems*.

Sun Y., Pang J.H.L. 2008. Digital image correlation for solder joint fatigue reliability in microelectronics packages. *Microelectronics Reliability* 48: 310 – 318.

Tee T.Y., Ng H.S., Yap D., Baraton X., Zhong Z. 2003. Board level solder joint reliability modelling and testing of TFBGA packages for telecommunication applications. *Microelectronics Reliability* 43: 1117 – 1123.

Trebuňa F., Huňady R., Bobovský Z., Hagara M. 2013. Results and experiences from the application of digital image correlation in operational modal analysis, *Acta Polytechnica Hungarica* 10(5): 159 – 174.

Zhang Z., Zhang W., Zhai Z.Z., Chen. Q.Y. 2007. Evaluation of various turbulence models in predicting airflow and turbulence in enclosed environments by CFD: Part 2 – Comparison with experimental data from literature. *HVAC&R Research* 13(6): 871 – 886.